

Isospin Breaking in Low-Energy Charged Pion and Kaon Elastic Scattering

A. Nehme¹

*Centre de Physique Théorique
CNRS-Luminy, case 907
F-13288 Marseille Cedex 09, France.*

Abstract

We use chiral perturbation theory to evaluate the scattering amplitude for the process $\pi^+K^- \rightarrow \pi^+K^-$ at leading and next-to-leading orders in the chiral counting and in the presence of isospin breaking effects. We also discuss the influence of the latter on the combination of the S -wave πK scattering lengths which is relevant for the $2S - 2P$ energy levels shift of $K\pi$ atoms.

Keywords: Electromagnetic corrections, Scattering lengths, Pion kaon scattering, Chiral perturbation theory

¹nehme@cpt.univ-mrs.fr

Contents

1	Introduction	2
2	Charged pion and kaon elastic scattering	3
3	Scattering lengths	6
4	Isospin violation at NLO	8
5	Conclusions	13
A	Scattering amplitude	13
B	Loop functions	19

1 Introduction

The study of hadronic atoms has become a very active field. Many experiments are devoted to measure the characteristics of such atoms with high precision [1, 2, 3, 4, 5]. These experimental results carry a theoretical interest since they permit a direct access to hadronic scattering lengths providing, in this way, valuable informations concerning the fundamental properties of QCD at low energy. For instance, the presently running DIRAC experiment aims at measuring the ponium lifetime τ with 10% accuracy [1]. This would allow one to determine the difference $a_0^0 - a_0^2$ with 5% precision by means of the Deser-type [6] relation [7]

$$\tau^{-1} \propto (a_0^0 - a_0^2)^2, \quad (1.1)$$

where a_l^I denotes the l -wave $\pi\pi$ scattering length in the channel with total isospin I . On the other hand, chiral perturbation theory (ChPT) [8, 9, 10] predictions for the scattering lengths have reached a precision amounting to 2% [11]. Once the final results from DIRAC are available, ChPT will therefore be subjected to a serious test. Before confronting the experimental determination to the ChPT prediction, it is desirable to get all sources of corrections to the relation (1.1), valid in the absence of isospin breaking, under control. In this direction, bound states calculations were performed using different approaches, like potential scattering theory [12, 13], 3D-constraint field theory [14], Bethe-Salpeter equation [15] and non-relativistic effective lagrangians [16, 17]. For a review on the subject and a comparison between the various methods we refer the reader to [18]. Within the framework of non-relativistic effective lagrangians, the correct expression of relation (1.1) which include all isospin breaking effects at leading order (LO) and next-to-leading order (NLO) was found in [19] to be

$$\tau^{-1} = \frac{1}{9} \alpha^3 (4M_{\pi^\pm}^2 - 4M_{\pi^0}^2 - M_{\pi^\pm}^2 \alpha^2)^{\frac{1}{2}} \mathcal{A}^2 (1 + K). \quad (1.2)$$

In the preceding equation, α stands for the fine-structure constant, \mathcal{A} and K possess the following expansions [19] in powers of the isospin breaking parameter $\kappa \in [\alpha, (m_d - m_u)^2]$

$$\mathcal{A} = -\frac{3}{32\pi} \text{Re} A_{\text{thr.}}^{+;-;00} + o(\kappa), \quad (1.3)$$

$$K = \frac{1}{9} \left(\frac{M_{\pi^\pm}^2}{M_{\pi^0}^2} - 1 \right) (a_0^0 + 2a_0^2)^2 - \frac{2\alpha}{3} (\ln \alpha - 1) (2a_0^0 + a_0^2) + o(\kappa). \quad (1.4)$$

The quantity of interest,

$$-\frac{3}{32\pi} \text{Re} A_{\text{thr.}}^{+-;00} = a_0^0 - a_0^2 + h_1(m_d - m_u)^2 + h_2\alpha, \quad (1.5)$$

represents the real part of the $\pi^+\pi^- \rightarrow \pi^0\pi^0$ scattering amplitude at order κ , calculated at threshold within ChPT to any chiral order and from which we subtract the singular pieces behaving like q^{-1} and $\ln q$ with q being the centre-of-mass three-momentum. While h_1 vanishes, the coefficient h_2 was calculated in [20] at $\mathcal{O}(e^2p^2)$ where p stands for a typical external momentum and e for the electric charge.

In the first DIRAC proposal [1], it was also planned to measure the ponium $2S - 2P$ energy levels shift ΔE . The possibility to perform such a measurement was discussed in [21]. A simultaneous measurement of τ and ΔE would allow to pin down a_0^0 and a_0^2 separately, since [22]

$$\Delta E \propto 2a_0^0 + a_0^2. \quad (1.6)$$

Bound states calculation of the isospin breaking corrections to (1.6) were done in [13] using potential scattering theory. Non-relativistic effective lagrangian calculations concerning ΔE are not available. One might however expect that they will involve the quantity $\text{Re} A_{\text{thr.}}^{+-;+-}$ for the corresponding $\pi^+\pi^- \rightarrow \pi^+\pi^-$ process. Electromagnetic corrections to the scattering amplitude for the process in question have been obtained at $\mathcal{O}(e^2p^2)$ in [23].

The proposal [1] was followed by another one extending the DIRAC project by considering the possibility of measuring the characteristics of $K\pi$ atoms with 20% accuracy [5]. The determination of the lifetime and energy levels shift for $K\pi$ atoms will give access to the S -wave πK scattering lengths $a_0^{1/2}$ and $a_0^{3/2}$ allowing to test ChPT in the three-flavor sector. Likewise, it is to be expected that the relevant quantities in the final expressions for the lifetime and the levels shift will involve the scattering amplitudes for $\pi^-K^+ \rightarrow \pi^0K^0$ and $\pi^+K^- \rightarrow \pi^+K^-$ respectively. In the case of the former, isospin breaking corrections have already been discussed in [24, 25]. The aim of the present work is to provide a similar treatment for the latter.

The paper is organized as follows. In Sec. 2, the scattering amplitude for the process $\pi^+K^- \rightarrow \pi^+K^-$ will be calculated at NLO including isospin breaking effects and ignoring the emission of real soft photons. Being lengthy, the expression for the scattering amplitude is displayed in App. A. We pursue with Sec. 3 where the analytic expressions for $a_0^{1/2}$ and $a_0^{3/2}$ at NLO are given. We then discuss the sensitivity of the scattering lengths to the size of the next-to-next-to leading order (NNLO) by evaluating them using various inputs for the low-energy constants (LEC's). The threshold expansion of the process in question is performed in Sec. 4 where the effects of isospin breaking on the scattering lengths are evaluated. Finally, App. B collects the expressions for the loop functions needed in the calculation.

2 Charged pion and kaon elastic scattering

The elastic scattering process

$$\pi^+(p_+) + K^-(k_-) \rightarrow \pi^+(p'_+) + K^-(k'_-), \quad (2.1)$$

is studied in terms of the Lorentz invariant Mandelstam variables

$$s = (p_+ + k_-)^2, \quad t = (p_+ - p'_+)^2, \quad u = (p_+ - k'_-)^2,$$

verifying the on-shell relation $s + t + u = 2(M_{\pi^\pm}^2 + M_{K^\pm}^2)$. These variables are related to the centre-of-mass three momentum q and scattering angle θ by

$$\begin{aligned} s &= \left(\sqrt{M_{\pi^\pm}^2 + q^2} + \sqrt{M_{K^\pm}^2 + q^2} \right)^2, \\ t &= -2q^2(1 - \cos\theta), \\ u &= \left(\sqrt{M_{\pi^\pm}^2 + q^2} - \sqrt{M_{K^\pm}^2 + q^2} \right)^2 - 2q^2(1 + \cos\theta). \end{aligned} \quad (2.2)$$

Let $\mathcal{M}^{+;-+}$ and $\mathcal{M}^{++;++}$ denote the respective scattering amplitudes for the process (2.1) and its crossed channel reaction $\pi^+ K^+ \rightarrow \pi^+ K^+$. Then, in the isospin limit, defined by the vanishing of both the electric charge e and the up and down quarks masses difference ($m_u = m_d, e = 0$), the following relations hold

$$\begin{aligned} \mathcal{M}^{+;-+}(s, t, u) &= \frac{2}{3} T^{1/2}(s, t, u) + \frac{1}{3} T^{3/2}(s, t, u), \\ \mathcal{M}^{++;++}(s, t, u) &= T^{3/2}(s, t, u), \end{aligned} \quad (2.3)$$

with T^I ($I = 1/2, 3/2$) being the isospin amplitudes. The processes under consideration are related by $s \leftrightarrow u$ crossing which constrains the T^I by

$$2T^{1/2}(s, t, u) = 3T^{3/2}(u, t, s) - T^{3/2}(s, t, u). \quad (2.4)$$

This is no more valid when isospin breaking effects, generated by $\delta = m_d - m_u$ and $\alpha = e^2/(4\pi)$ are switched on. In this case $s \leftrightarrow u$ crossing is expressed as

$$\mathcal{M}^{+;-+}(s, t, u) = \mathcal{M}^{++;++}(u, t, s). \quad (2.5)$$

The effect of a non-zero value for δ can be analyzed fully by means of the strong sector chiral lagrangian constructed in [26]. Treating isospin violation of electromagnetic origin requires the extension of ChPT in order to include virtual photons. This can be done by building operators in which photons figure as explicit dynamical degrees of freedom. The electromagnetic sector chiral lagrangian, founded upon the chiral counting scheme $\mathcal{O}(e) = \mathcal{O}(p)$, was presented at NLO in [27] and [28].

We shall calculate the scattering amplitude (2.5) at NLO including isospin breaking effects of both strong and electromagnetic origin. Consistency demands that all of the following chiral orders should be present; $p^2, e^2, \delta, p^4, e^2 p^2, \delta p^2, e^4, \delta e^2, \delta^2$. From naïve dimensional estimation, we believe that the last three orders are beyond the accuracy we ask for and hence will be ignored in the following. Furthermore instead of δ , our results will be expressed in terms of [26]

$$\epsilon \equiv \frac{\sqrt{3}}{4} \frac{m_d - m_u}{m_s - \hat{m}} = 1.00 \cdot 10^{-2},$$

which measures the rate of isospin violation with respect to the violation of $SU(3)$. Using Feynman graph techniques, the amplitude (2.5) can be represented at NLO by the one-particle-irreducible diagrams depicted in Fig. 1.

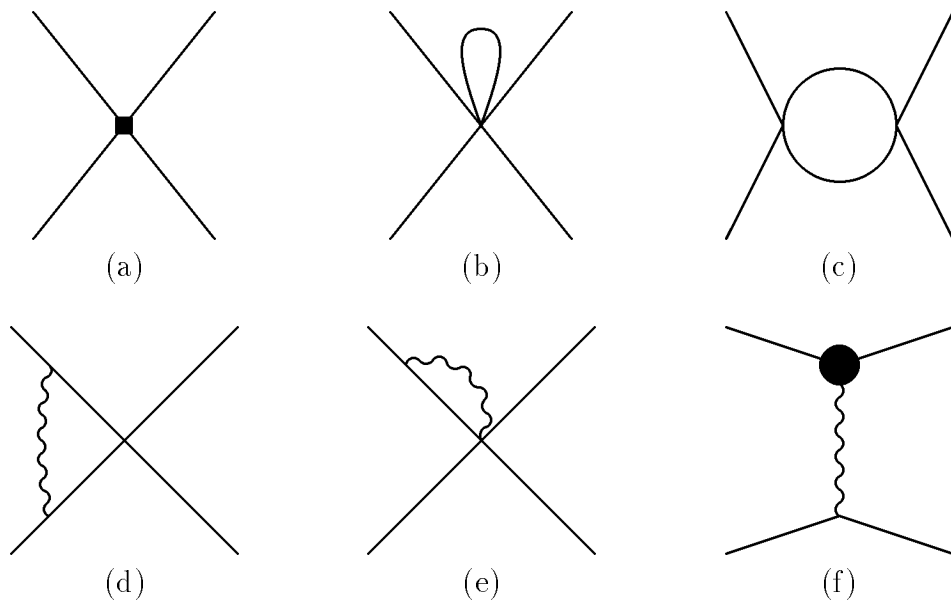


Figure 1: The various types of Feynman diagrams encountered in the charged πK scattering to one-loop order and ignoring $\mathcal{O}(e^4)$. The born-type diagram is represented by (a). Besides the contribution from the LEC's (the full square), it contains the tree contribution including the effects of bare masses and wave functions renormalization. Diagram (b) represents the tadpole-type part of the amplitude. The s -, t - and u -channel parts are schematized by diagram (c) and its crossed. The one-photon contribution to the amplitude follows from diagrams (d) and (e). We refer to diagram (f) as the form-factor-type where the full circle is made explicit in Fig. 2.

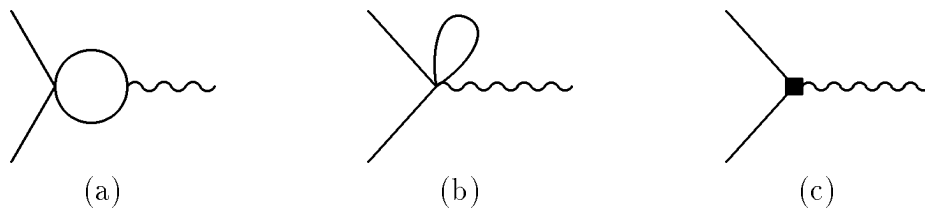


Figure 2: The electromagnetic vertex function of a charged meson to one-loop order. The full square takes into account the contribution from the LEC's just as the tree contribution including the effect of wave function renormalization. Are shown only diagrams of $\mathcal{O}(ep^3)$.

Although the evaluation of these diagrams is a simple exercise in quantum field theory, it involves different masses, yielding, in that manner, lengthy expressions. These are displayed in App. A where we keep the contributions of the various diagrams separated. It is useful to mention, at this stage, that these expressions are scale independent but infrared divergent. Since only observables are infrared safe, these infrared divergencies should cancel in the expression for the cross section where not only virtual photons but also real soft photons have to be taken into account. The $\mathcal{O}(\alpha)$ soft photon cross section corresponding to an arbitrary matrix element was calculated in [29]. We checked that by applying the general formula derived in that reference to the present case, the terms in $\ln m_\gamma$ so obtained cancel with the ones coming from our expressions.

3 Scattering lengths

We are interested by the S -wave πK scattering lengths [30, 31, 32]. To this end, it is convenient to introduce the partial wave amplitudes t_l^I defined in the s -channel by

$$T^I(s, \cos \theta) = 32\pi \sum_l (2l + 1) P_l(\cos \theta) t_l^I(s), \quad (3.1)$$

where l is the angular momentum of the πK system and the P_l 's are the Legendre polynomials. Near threshold the partial wave amplitudes can be parametrized in terms of the scattering lengths a_l^I and slope parameters b_l^I . In the normalization (3.1), the real part of the partial wave amplitudes reads

$$\text{Re } t_l^I(s) = q^{2l} [a_l^I + b_l^I q^2 + \mathcal{O}(q^4)]. \quad (3.2)$$

At NLO in ChPT no analytic expressions for the scattering lengths exist in the literature. This is not the case in other approaches such as heavy-kaon ChPT [33] where the expansion parameter is M_π/M_K in addition to $M_\pi/(4\pi F_0)$ or $M_K/(4\pi F_0)$ for ChPT². Obviously, at any order in both expansions, a matching between the two approaches is feasible. Getting analytic expressions for $a_0^{1/2}$ and $a_0^{3/2}$ is a straightforward matter. Using the expression of the isospin amplitude $T^{3/2}$ given in [34], Eqs. (2.2)-(2.4) together with (3.1) and (3.2) lead the following NLO expressions for the scattering lengths

$$\begin{aligned} 32\pi a_0^{1/2} &= \frac{2M_{\pi^\pm} M_{K^\pm}}{F_\pi F_K} \left\{ 1 + \frac{4}{F_\pi F_K} (M_{\pi^\pm}^2 + M_{K^\pm}^2) L_5^r \right. \\ &- \frac{1}{1152\pi^2 F_\pi F_K} \frac{1}{M_{K^\pm}^2 - M_{\pi^\pm}^2} \left[9M_{\pi^\pm}^2 (11M_{K^\pm}^2 - 5M_{\pi^\pm}^2) \ln \frac{M_{\pi^\pm}^2}{\mu^2} \right. \\ &+ 2M_{K^\pm}^2 (9M_{K^\pm}^2 - 55M_{\pi^\pm}^2) \ln \frac{M_{K^\pm}^2}{\mu^2} + (36M_{K^\pm}^4 + 11M_{K^\pm}^2 M_{\pi^\pm}^2 - 9M_{\pi^\pm}^4) \ln \frac{M_\eta^2}{\mu^2} \left. \right\} \\ &+ \frac{M_{\pi^\pm}^2 M_{K^\pm}^2}{576\pi^2 F_\pi^2 F_K^2} \left\{ 172 + 576\pi^2 \mathcal{B}(M_{K^\pm}, M_{\pi^\pm}) - 192\pi^2 \mathcal{B}(M_{K^\pm}, -M_{\pi^\pm}) \right. \\ &+ 4608\pi^2 [4(L_1^r + L_2^r) + 2(L_3 - 2L_4^r) - L_5^r + 2(2L_6^r + L_8^r)] + \frac{1}{M_{K^\pm}^2 - M_{\pi^\pm}^2} \times \end{aligned}$$

²All along this paper, M_π and M_K represent respectively the pion and kaon masses in the isospin limit, M_η the eta mass, F_0 the coupling of Goldstone bosons to axial currents in the chiral limit.

$$\begin{aligned}
32\pi a_0^{3/2} = & \left[99M_{\pi^\pm}^2 \ln \frac{M_{\pi^\pm}^2}{\mu^2} - 2(67M_{K^\pm}^2 - 8M_{\pi^\pm}^2) \ln \frac{M_{K^\pm}^2}{\mu^2} + (24M_{K^\pm}^2 - 5M_{\pi^\pm}^2) \ln \frac{M_\eta^2}{\mu^2} \right] \Big\}, \\
& - \frac{M_{\pi^\pm} M_{K^\pm}}{F_\pi F_K} \left\{ 1 + \frac{4}{F_\pi F_K} (M_{\pi^\pm}^2 + M_{K^\pm}^2) L_5^r \right. \\
& - \frac{1}{1152\pi^2 F_\pi F_K} \frac{1}{M_{K^\pm}^2 - M_{\pi^\pm}^2} \left[9M_{\pi^\pm}^2 (11M_{K^\pm}^2 - 5M_{\pi^\pm}^2) \ln \frac{M_{\pi^\pm}^2}{\mu^2} \right. \\
& + 2M_{K^\pm}^2 (9M_{K^\pm}^2 - 55M_{\pi^\pm}^2) \ln \frac{M_{K^\pm}^2}{\mu^2} + (36M_{K^\pm}^4 + 11M_{K^\pm}^2 M_{\pi^\pm}^2 - 9M_{\pi^\pm}^4) \ln \frac{M_\eta^2}{\mu^2} \Big] \Big\} \\
& + \frac{M_{\pi^\pm}^2 M_{K^\pm}^2}{576\pi^2 F_\pi^2 F_K^2} \left\{ 172 + 384\pi^2 \mathcal{B}(M_{K^\pm}, -M_{\pi^\pm}) \right. \\
& + 4608\pi^2 [4(L_1^r + L_2^r) + 2(L_3 - 2L_4^r) - L_5^r + 2(2L_6^r + L_8^r)] + \frac{1}{M_{K^\pm}^2 - M_{\pi^\pm}^2} \times \\
& \left. \left[99M_{\pi^\pm}^2 \ln \frac{M_{\pi^\pm}^2}{\mu^2} - 2(67M_{K^\pm}^2 - 8M_{\pi^\pm}^2) \ln \frac{M_{K^\pm}^2}{\mu^2} + (24M_{K^\pm}^2 - 5M_{\pi^\pm}^2) \ln \frac{M_\eta^2}{\mu^2} \right] \right\}.
\end{aligned} \tag{3.3}$$

The preceding expressions were obtained by using, in the NLO contributions, the Gell–Mann–Okubo relation (4.5) in the isospin limit [35]. F_π and F_K stand for the pion and kaon decay constants respectively. Their NLO expressions in the isospin limit can be found in [26]. For their numerical values we will use $F_\pi = 92.4 \text{ MeV}$ [36] and $F_K = 1.22F_\pi$ [37, 38]. The L_i 's are the LEC's weighting $\mathcal{O}(p^4)$ operators in the effective lagrangian of [26] and whose values are collected in Tab. 1 with various experimental determinations. Finally, for compactness, we introduced the function \mathcal{B} whose expression is displayed in App. B. For historical reasons [30], the scattering lengths were defined in terms of the charged pion and kaon masses ($M_{\pi^\pm} = 139.570 \text{ MeV}$, $M_{K^\pm} = 493.677 \text{ MeV}$). Furthermore, F_0^2 was renormalized as $F_\pi F_K$ instead of F_π^2 . Nevertheless, if one wishes to adopt the second choice for the renormalization of F_0 , the isospin limit of Eq. (4.7) can be used.

	set I	set II	set III
$10^3 L_1^r(M_\rho)$	0.46 ± 0.23	0.53 ± 0.25	0.43 ± 0.12
$10^3 L_2^r(M_\rho)$	1.49 ± 0.23	0.71 ± 0.27	0.73 ± 0.12
$10^3 L_3^r(M_\rho)$	-3.18 ± 0.85	-2.72 ± 1.12	-2.35 ± 0.37
$10^3 L_4^r(M_\rho)$	0 ± 0.5	0 ± 0.5	0 ± 0.5
$10^3 L_5^r(M_\rho)$	1.46 ± 0.2	0.91 ± 0.15	0.97 ± 0.11
$10^3 L_6^r(M_\rho)$	0 ± 0.3	0 ± 0.3	0 ± 0.3
$10^3 L_8^r(M_\rho)$	1.00 ± 0.20	0.62 ± 0.20	0.60 ± 0.18

Table 1: Values of the L_i^r 's obtained in [39] by using large N_c arguments [40] and fitting data from [41] to ChPT predictions at NLO (set I) as also at NNLO (set II). Set III is the equivalent of set II with data coming from the preliminary analysis [42] of the E865 experiment.

We applied several checks to expressions (3.3). They are scale independent, the scale dependence μ of the chiral logarithms is compensated by the one governing the renormalization group equations [26] of the running couplings $L_i^r(\mu) \equiv L_i^r$. Even so, all of our expressions will be evaluated at the scale $\mu = M_\rho = 770 \text{ MeV}$. Expanding expressions (3.3) to the fourth order in

powers of M_{π^\pm}/M_{K^\pm} we recover the combinations of scattering lengths obtained within the framework of heavy-kaon ChPT [33]. Using the same inputs as in [34] we found again their numerical estimates. These expressions are consistent analytically and numerically with the combinations $2a_0^{3/2} + a_0^{1/2}$ and $a_0^{1/2} - a_0^{3/2}$ evaluated in [24].

F_0 renormalization	a_0^I	set I	set II	set III
$F_0^2 = F_\pi^2$	$a_0^{1/2}$	0.214 ± 0.016	0.202 ± 0.018	0.203 ± 0.013
	$a_0^{3/2}$	-0.0557 ± 0.0166	-0.0660 ± 0.0185	-0.0644 ± 0.0133
$F_0^2 = F_\pi F_K$	$a_0^{1/2}$	0.192 ± 0.011	0.177 ± 0.012	0.179 ± 0.009
	$a_0^{3/2}$	-0.0613 ± 0.0113	-0.0651 ± 0.0125	-0.0644 ± 0.0090

Table 2: ChPT predictions for the S -wave πK scattering lengths at NLO with two possible renormalization choices for F_0 . Set I, set II and set III are defined in Table 1.

We shall now update the numerical evaluation of [34] for the scattering lengths. All inputs have been given exception of the eta mass to which we assign the value $M_\eta = 547.30$ MeV. We will evaluate $a_0^{1/2}$ and $a_0^{3/2}$ using each of the sets defined in Tab. 1 with both renormalization choices for F_0^2 . The interest behind this is the following. Since the difference between F_π and F_K in the NLO pieces is of $\mathcal{O}(p^6)$, then any difference in the values for the scattering lengths due to the renormalization choice for F_0 could be viewed as an indication for the size of the NNLO corrections. With respect to the different sets of Tab. 1, set I and set II were obtained by fitting respectively the same experimental data to one- and two-loop ChPT predictions. It follows that the possible variation in the values for the scattering lengths due to the use of either the two sets measures the influence of the NNLO on the NLO which, in a way, reflects the rate of convergence of the chiral expansion in powers of m_s . While Table 2 collects our numerical results for the scattering lengths, we will concentrate on two specific combinations, $2a_0^{1/2} + a_0^{3/2}$ and $a_0^{1/2} - a_0^{3/2}$. For the latter, the variations are about $\sim 9\%$ due to the renormalization choice for F_0 and $\sim 1\%$ ($\sim 5\%$) due to the choice of set II instead of set I with $F_0^2 = F_\pi^2$ ($F_0^2 = F_\pi F_K$). With regard to the former, the renormalization choice for F_0 induces about $\sim 17\%$ of variation versus $\sim 10\%$ due to the choice of the set for both renormalization choices. Notice that up to 10% of accuracy, the combination $a_0^{1/2} - a_0^{3/2}$ is altered neither by the renormalization choice for F_0 nor by the choice between set I and set II. This result has already been noticed in [24] where it was concluded that the theoretical prediction for $a_0^{1/2} - a_0^{3/2}$ is so clean that if the combination in question is measured accurately, the validity of standard three-flavor ChPT can be confirmed or not.

4 Isospin violation at NLO

The scattering lengths are well-defined quantities in the absence of radiative corrections. When virtual photons effects have to be taken into account, things must be handled with care. To prevent any confusion, we will perform step by step the threshold expansion of the amplitude

(2.5) with the help of Apps. A and B. When expanded in powers of q , the real part of (2.5) can be put in an analogous form as for the $\pi\pi$ scattering case [20]

$$\text{Re } \mathcal{M}^{+-;+-}(s, t, u) = \frac{M_{\pi^\pm} M_{K^\pm}}{F_\pi F_K} \frac{e^2}{4} \frac{\mu_{\pi K}}{q} + e^2 \left(\frac{u-s}{t} \right) + \text{Re } \mathcal{M}_{\text{thr.}}^{+-;+-} + \mathcal{O}(q), \quad (4.1)$$

$$\text{Re } \mathcal{M}^{++;++}(s, t, u) = \frac{M_{\pi^\pm} M_{K^\pm}}{F_\pi F_K} \frac{e^2}{4} \frac{\mu_{\pi K}}{q} + e^2 \left(\frac{s-u}{t} \right) + \text{Re } \mathcal{M}_{\text{thr.}}^{++;++} + \mathcal{O}(q). \quad (4.2)$$

The first two terms in the right-hand side of equation (4.1) should be absorbed in the static characteristics of $K\pi$ atoms [43, 44, 45] by means of a bound states treatment. The term in q^{-1} is due to the Coulomb photon exchanged between the scattered particles in diagram (d) of Fig. 1. As to the term where the dependence on the Mandelstam variables is kept explicit, it corresponds to diagram (f) of Fig. 1 at tree level and contains, besides the dependence on θ , a singular piece behaving like q^{-2} . The q - and θ -independent terms, $\text{Re } \mathcal{M}_{\text{thr.}}^{+-;+-}$ and $\text{Re } \mathcal{M}_{\text{thr.}}^{++;++}$, constitute the central object of the current work. Their isospin limit is nothing else than the threshold value of equation (2.3). Then, in order to keep a coherent notation, they will be denoted in the following by

$$\text{Re } \mathcal{M}_{\text{thr.}}^{+\mp;+\mp} = 32\pi a_0(+\mp; +\mp),$$

where

$$\begin{aligned} a_0(+--;+-) &= \frac{1}{3} \left(2a_0^{1/2} + a_0^{3/2} \right) + \Delta a_0(+--;+-), \\ a_0(++;++) &= a_0^{3/2} + \Delta a_0(++;++), \end{aligned} \quad (4.3)$$

and the NLO expressions (3.3) were used for $a_0^{1/2}$ and $a_0^{3/2}$. Let us turn towards the calculation of the isospin breaking quantities Δa_0 . To begin with, we express the isospin limit masses M_π and M_K figuring at NLO in terms of the charged and neutral ones by means of

$$M_\pi^2 \rightarrow M_{\pi^0}^2, \quad 2M_K^2 \rightarrow M_{K^\pm}^2 + M_{K^0}^2 - \gamma(M_{\pi^\pm}^2 - M_{\pi^0}^2), \quad (4.4)$$

where γ takes into account any deviation from Dashen's theorem [46] for which $\gamma = 1$. Although our results correspond to $\gamma = 1$, we will use the value $\gamma = 1.84$ [47] as an indicator for their sensitivity to the violation of Dashen theorem [48]. Furthermore, for simplification, the modified Gell–Mann–Okubo relation

$$3M_\eta^2 \rightarrow 2(M_{K^\pm}^2 + M_{K^0}^2) - (2M_{\pi^\pm}^2 - M_{\pi^0}^2), \quad (4.5)$$

will be used everywhere except in the arguments of the chiral logarithms where the eta mass is assigned to its physical value. Nevertheless, the effect, on the final results, of ignoring Eq. (4.5) will be also considered. Next, since by convention, the isospin limit is defined in terms of the charged pion and kaon masses, the neutral ones should be replaced according to

$$M_{\pi^0}^2 \rightarrow M_{\pi^\pm}^2 - \Delta_\pi, \quad M_{K^0}^2 \rightarrow M_{K^\pm}^2 - \Delta_K.$$

The advantage of such a procedure is that, when expanding a_0 in powers of Δ_π and Δ_K , the zero-th order in the expansion is automatically defined in terms of the charged masses and reproduces the expression for the corresponding combination of scattering lengths as given by (4.3) and (3.3). Although sufficient for our purposes, the expansion to first order in Δ_π and Δ_K

is somewhat tedious especially at the level of the loop functions. The corresponding expansions of the latter are collected in App. B. Having all this, the last step is achieved by replacing Δ_π and Δ_K in the NLO terms by their LO expressions

$$\Delta_\pi \rightarrow 2Z_0 e^2 F_0^2, \quad \Delta_K \rightarrow 2Z_0 e^2 F_0^2 - \frac{4\epsilon}{\sqrt{3}} (M_K^2 - M_\pi^2),$$

which permit the following decomposition

$$\begin{aligned} 32\pi \Delta a_0(+--;+-) &\equiv \frac{\Delta_\pi}{F_\pi F_K} + \frac{\epsilon}{\sqrt{3}} \delta_\epsilon^{+-;+-} + 2Z_0 e^2 F_0^2 \delta_{Z_0 e^2}^{+-;+-} + e^2 \delta_{e^2}^{+-;+-}, \\ 32\pi \Delta a_0(++;++) &\equiv \frac{\Delta_\pi}{F_\pi F_K} + \frac{\epsilon}{\sqrt{3}} \delta_\epsilon^{++;++} + 2Z_0 e^2 F_0^2 \delta_{Z_0 e^2}^{++;++} + e^2 \delta_{e^2}^{++;++}. \end{aligned} \quad (4.6)$$

Once more, the renormalization choice for F_0 was fixed to $F_0^2 = F_\pi F_K$ with the possibility of renormalizing as $F_0^2 = F_\pi^2$ offered by the relation

$$\begin{aligned} \frac{1}{F_\pi F_K} &= \frac{1}{F_\pi^2} \left\{ 1 + \frac{4}{F_\pi^2} (M_{\pi^\pm}^2 - M_{K^\pm}^2) L_5^r \right. \\ &- \frac{1}{128\pi^2 F_\pi^2} \left[5M_{\pi^\pm}^2 \ln \frac{M_{\pi^\pm}^2}{\mu^2} - 2M_{K^\pm}^2 \ln \frac{M_{K^\pm}^2}{\mu^2} - (4M_{K^\pm}^2 - M_{\pi^\pm}^2) \ln \frac{M_\eta^2}{\mu^2} \right] \\ &- \frac{\Delta_\pi}{F_\pi^2} \left[2L_5^r - \frac{1}{128\pi^2} \left(4 + 5 \ln \frac{M_\pi^2}{\mu^2} - \ln \frac{M_K^2}{\mu^2} - \ln \frac{M_\eta^2}{\mu^2} \right) \right] \\ &\left. + \frac{\Delta_K}{F_\pi^2} \left[2L_5^r - \frac{1}{128\pi^2} \left(1 + \ln \frac{M_K^2}{\mu^2} + 2 \ln \frac{M_\eta^2}{\mu^2} \right) \right] \right\}. \end{aligned} \quad (4.7)$$

Notice that the consistency of the chiral power counting scheme requires that the mesons masses appearing in (4.6) be set to their isospin limit; the difference being of higher order, thus, beyond the accuracy needed for the present work.

The isospin breaking term in (4.6) generated by the difference between m_u and m_d is given by

$$\begin{aligned} \delta_\epsilon^{+\mp;+\mp} &= \mp \frac{M_\pi M_K}{288\pi^2 F_\pi^2 F_K^2} \left\{ -2304\pi^2 (M_K^2 - M_\pi^2) L_5^r \right. \\ &+ \frac{1}{4M_K^2 - M_\pi^2} [36M_K^4 + 563M_\pi^2 M_K^2 - 135M_\pi^4 - 576\pi^2 M_\pi^2 M_K^2 \mathcal{B}(M_K, \pm M_\pi)] \\ &+ \frac{1}{M_K^2 - M_\pi^2} \left[27M_\pi^2 (8M_K^2 + M_\pi^2) \ln \frac{M_\pi^2}{\mu^2} \right. \\ &+ \left. (9M_K^4 - 274M_\pi^2 M_K^2 + 9M_\pi^4) \ln \frac{M_K^2}{\mu^2} + (18M_K^4 + 4M_\pi^2 M_K^2 - 9M_\pi^4) \ln \frac{M_\eta^2}{\mu^2} \right] \left. \right\} \\ &+ \frac{M_\pi^2 M_K^2}{288\pi^2 F_\pi^2 F_K^2} \left\{ \frac{8}{4M_K^2 - M_\pi^2} [68M_K^2 - 19M_\pi^2 - 12\pi^2 (32M_K^2 - 5M_\pi^2) \mathcal{B}(M_K, \pm M_\pi)] \right. \\ &+ \frac{1}{M_K^2 - M_\pi^2} \left[9(6M_K^2 + 19M_\pi^2) \ln \frac{M_\pi^2}{\mu^2} \right. \\ &\left. \left. - 128(M_K^2 + M_\pi^2) \ln \frac{M_K^2}{\mu^2} + (74M_K^2 - 43M_\pi^2) \ln \frac{M_\eta^2}{\mu^2} \right] \right\}. \end{aligned} \quad (4.8)$$

The isospin violating term due to the electromagnetic difference between charged and neutral mesons masses squared was found to be

$$\begin{aligned}
\delta_{Z_0 e^2}^{+\mp;+\mp} &= \pm \frac{M_\pi M_K}{1152\pi^2 F_\pi^2 F_K^2} \left\{ 471\delta_{+\mp} \right. \\
&- 768\pi^2 [12L_5^r - \mathcal{B}(M_K, \pm M_\pi)] - \frac{64M_K^2}{4M_K^2 - M_\pi^2} [1 - 18\pi^2 \mathcal{B}(M_K, \pm M_\pi)] \\
&+ \frac{1}{M_K^2 - M_\pi^2} \left[-471\Delta_{\pi K} \delta_{-\mp} - 38M_K^2 - 288\pi^2 M_K^2 \mathcal{B}(M_K, \pm M_\pi) \right. \\
&+ 27(M_K^2 + 9M_\pi^2) \ln \frac{M_\pi^2}{\mu^2} - 2(161M_K^2 + 11M_\pi^2) \ln \frac{M_K^2}{\mu^2} + (43M_K^2 + 31M_\pi^2) \ln \frac{M_\eta^2}{\mu^2} \left. \right] \left. \right\} \\
&+ \frac{1}{1152\pi^2 F_\pi^2 F_K^2} \frac{M_\pi^2 M_K^2}{M_K^2 - M_\pi^2} \left[78 + 9216\pi^2 L_5^r \right. \\
&- 864\pi^2 \mathcal{B}(M_K, \pm M_\pi) + 81 \ln \frac{M_\pi^2}{\mu^2} + 110 \ln \frac{M_K^2}{\mu^2} - 11 \ln \frac{M_\eta^2}{\mu^2} \left. \right] \\
&- \frac{1}{1152\pi^2 F_\pi^2 F_K^2} \frac{M_\pi^4}{M_K^2 - M_\pi^2} \left[64 \right. \\
&+ 9216\pi^2 [2L_4^r + L_5^r - 2(2L_6^r + L_8^r)] + 63 \ln \frac{M_\pi^2}{\mu^2} - 5 \ln \frac{M_\eta^2}{\mu^2} \left. \right] \\
&- \frac{M_K^4}{576\pi^2 F_\pi^2 F_K^2} \left\{ \frac{64}{4M_K^2 - M_\pi^2} [1 + 18\pi^2 \mathcal{B}(M_K, \pm M_\pi)] - \frac{1}{M_K^2 - M_\pi^2} [12 \right. \\
&+ 9216\pi^2 (L_4^r - 2L_6^r - L_8^r) + 288\pi^2 \mathcal{B}(M_K, \pm M_\pi) - 27 \ln \frac{M_K^2}{\mu^2} - 34 \ln \frac{M_\eta^2}{\mu^2} \left. \right] \left. \right\}, \quad (4.9)
\end{aligned}$$

with δ_{ij} representing the Kronecker symbol. Finally, virtual photons induce the following correction

$$\begin{aligned}
\delta_{e^2}^{+\mp;+\mp} &= \pm \frac{M_\pi M_K}{144\pi^2 F_\pi F_K} \frac{1}{M_K^2 - M_\pi^2} \left\{ 6[5M_K^2 + 11M_\pi^2 - 384\pi^2(M_K^2 - M_\pi^2)L_9^r] \right. \\
&- 128\pi^2 (M_K^2 - M_\pi^2) (3K_1^r + 3K_2^r - 18K_3^r - 9K_4^r + 4K_5^r - 5K_6^r) + \frac{3}{M_K^2 - M_\pi^2} \times \\
&\left[(11M_K^4 + 9M_K^2 M_\pi^2 + 12M_\pi^4) \ln \frac{M_\pi^2}{\mu^2} + (4M_K^4 - 39M_K^2 M_\pi^2 + 3M_\pi^4) \ln \frac{M_K^2}{\mu^2} \right] \left. \right\} \\
&- \frac{M_\pi^2 M_K^2}{16\pi^2 F_\pi F_K} \frac{1}{M_K^2 - M_\pi^2} \left\{ 36 - 32\pi^2 (2K_3^r - K_4^r - 4K_{10}^r - 4K_{11}^r) \right. \\
&+ \frac{1}{M_K^2 - M_\pi^2} \left[(9M_K^2 + 23M_\pi^2) \ln \frac{M_\pi^2}{\mu^2} - 5(3M_K^2 + 4M_\pi^2) \ln \frac{M_K^2}{\mu^2} \right] \left. \right\} \\
&+ \frac{2M_\pi^4}{3F_\pi F_K} \frac{1}{M_K^2 - M_\pi^2} (12K_2^r - 6K_3^r + 3K_4^r + K_5^r + 7K_6^r - 12K_8^r - 6K_{10}^r - 6K_{11}^r) \\
&+ \frac{M_K^4}{48\pi^2 F_\pi F_K} \frac{1}{M_K^2 - M_\pi^2} \left[12 \right. \\
&- 32\pi^2 (12K_2^r + K_5^r + 7K_6^r - 12K_8^r - 18K_{10}^r - 18K_{11}^r) - \frac{9M_K^2}{M_K^2 - M_\pi^2} \ln \frac{M_K^2}{\mu^2} \left. \right]. \quad (4.10)
\end{aligned}$$

It is important to stress that the virtual photons contribution, as can be seen from (4.10), is safe

from infrared divergencies. The dependence on m_γ appears at higher orders of the expansions (4.1) and (4.2) in power of q . This fact was already noticed in [20].

For the numerical estimation of the isospin breaking effects we use $M_{\pi^0}^2 = 134.976$ MeV, $M_{K^0}^2 = 497.672$ MeV and the values of the L_i^r 's corresponding to set II of Tab. 1 are our preferred ones. Concerning the LEC L_9 entering the expressions for the electromagnetic form factors of the pion and the kaon, its value will be taken as $L_9^r = (6.9 \pm 0.7) \cdot 10^{-3}$. With respect to the LEC's in the electromagnetic sector, their central values correspond to the ones quoted in [49] where large N_c arguments [40] and resonances saturation were applied to pin them down. Moreover, an uncertainty of $\pm 1/(16\pi^2)$, coming from naïve dimensional analysis, will be attributed to each of the K_i^r 's. In order to compare the order of magnitudes for the scattering lengths and the isospin breaking corrections to them at NLO we recall the following combinations from Tab. 2 corresponding to the renormalization choice $F_0^2 = F_\pi F_K$,

$$\frac{1}{3} \left(2a_0^{1/2} + a_0^{3/2} \right) = 0.096 \pm 0.012, \quad a_0^{3/2} = -0.0651 \pm 0.0125. \quad (4.11)$$

Having all this, we obtain for the process $\pi^- K^+ \rightarrow \pi^- K^+$ the following estimation for the isospin breaking effects

$$\begin{aligned} \frac{1}{32\pi} \quad \frac{\Delta_\pi}{F_\pi F_K} &= 1.2 \cdot 10^{-3}, \\ \frac{1}{32\pi} \quad \frac{\epsilon}{\sqrt{3}} \delta_\epsilon^{+-;+-} &= (2.3 \pm 0.1) \cdot 10^{-4}, \\ \frac{1}{32\pi} \quad 2Z_0 e^2 F_0^2 \delta_{Z_0 e^2}^{+-;+-} &= (1.4 \pm 3.9) \cdot 10^{-4}, \\ \frac{1}{32\pi} \quad e^2 \delta_{e^2}^{+-;+-} &= (-3.8 \pm 31) \cdot 10^{-4}. \end{aligned}$$

From this we deduce that

$$a_0(+--;+-) = 0.097 \pm 0.013, \quad (4.12)$$

indicating that the isospin breaking effects induce a correction on the combination $2a_0^{1/2} + a_0^{3/2}$ amounting to 1%. As for the process $\pi^+ K^+ \rightarrow \pi^+ K^+$, the results are

$$\begin{aligned} \frac{1}{32\pi} \quad \frac{\Delta_\pi}{F_\pi F_K} &= 1.2 \cdot 10^{-3}, \\ \frac{1}{32\pi} \quad \frac{\epsilon}{\sqrt{3}} \delta_\epsilon^{++;++} &= (-1.4 \pm 0.1) \cdot 10^{-4}, \\ \frac{1}{32\pi} \quad 2Z_0 e^2 F_0^2 \delta_{Z_0 e^2}^{++;++} &= (-3.3 \pm 3.9) \cdot 10^{-4}, \\ \frac{1}{32\pi} \quad e^2 \delta_{e^2}^{++;++} &= (12.7 \pm 31) \cdot 10^{-4}, \end{aligned}$$

and lead to

$$a_0(++;++) = -0.0631 \pm 0.0129. \quad (4.13)$$

Although the size of the correction on $a_0^{3/2}$ is slightly bigger ($\sim 3\%$), it is the former combination, (4.12), that is expected to enter the expression for the $2S - 2P$ energy levels shift for $K\pi$ atoms. Before concluding let us comment about the effect induced on these results by deviations from the Gell–Mann–Okubo relation and Dashen theorem. If one uses the physical eta mass instead of Eq. (4.5), the central value in (4.12) increases by ~ 0.0002 . On the other hand, variations of γ in (4.4) between 1 to 1.84 cause deviations of order $\sim 10^{-5}$. Accordingly, deviations from both Gell–Mann–Okubo relation and Dashen theorem induce corrections which are beyond the accuracy we ask for.

5 Conclusions

This work was devoted to the study at NLO of isospin breaking effects on the combination $2a_0^{1/2} + a_0^{3/2}$ of S -wave πK scattering lengths which is relevant for the $2S - 2P$ energy levels shift of $K\pi$ atoms. We first gave analytic expressions for the scattering lengths which allowed to evaluate them using several sets for the values of the LEC's and with both replacements $F_0^2 \rightarrow F_\pi F_K$ and $F_0^2 \rightarrow F_\pi^2$. The particularity of the sets in question is that set I and set II for instance were determined by fitting the same experimental data to one- and two-loop ChPT predictions. We obtained for the value of the afore-mentioned combination a variation amounting to $\sim 17\%$ due to the choice for the replacement of F_0^2 . As for the choice between the two sets, it induces $\sim 10\%$ variation. These numbers can be used as indicators for the size of the NNLO corrections as well as for the rate of convergence of the chiral expansion in powers of m_s . We pursued by performing, in parallel with what has been done for the $\pi\pi$ scattering case, the threshold expansion of the scattering amplitude for the process $\pi^+ K^- \rightarrow \pi^+ K^-$ in the presence of photons. After subtracting singular pieces, we evaluated the isospin breaking corrections to the combination in question and noticed two features of them: i) in spite of the fact that the NLO corrections of both strong and electromagnetic origin are bigger than the LO one, they cancel each others at the end. ii) Their central value represents $\sim 1\%$ of the NLO value for the combination $2a_0^{1/2} + a_0^{3/2}$ and the uncertainty embarrassing them is negligible with respect to the one coming from the LEC's in the strong sector.

Acknowledgements

The author is grateful to M. Knecht for suggesting this study, for constant encouragement, precious comments and valuable advices about both the content and the presentation of the document. The author wishes to thank H. Saizdjian for enjoyable discussions, P. Talavera for helpful and appreciated comments.

A Scattering amplitude

The amplitude (2.5) will be divided into seven parts depending on the nature of the corresponding Feynman diagrams

$$\mathcal{M}^{+-;+-} = \mathcal{M}^{\text{born}} + \mathcal{M}^{\text{tadpole}}$$

$$\begin{aligned}
& + \mathcal{M}^{\text{s-channel}} + \mathcal{M}^{\text{t-channel}} + \mathcal{M}^{\text{u-channel}} \\
& + \mathcal{M}^{\text{one-photon}} + \mathcal{M}^{\text{form factor}} .
\end{aligned} \tag{A.1}$$

We distinguish three contributions to the born part of the amplitude (diagram (a) in figure 1)

$$\mathcal{M}^{\text{born}} = \mathcal{M}_{\text{tree}}^{\text{born}} + \mathcal{M}_{p^4}^{\text{born}} + \mathcal{M}_{e^2 p^2}^{\text{born}} .$$

The tree contribution, denoted by $\mathcal{M}_{\text{tree}}^{\text{born}}$, accounts for the four-meson vertex derived from the leading order (LO) lagrangian. Bare masses and mesons wave functions being renormalized, the result is the following

$$\begin{aligned}
\mathcal{M}_{\text{tree}}^{\text{born}} &= \frac{1}{2F_0^2}(M_{\pi^\pm}^2 + M_{K^\pm}^2 - u) + \frac{\Delta_\pi}{F_0^2} \\
&+ \frac{1}{2F_0^2}(M_{\pi^\pm}^2 + M_{K^\pm}^2 - u) \left\{ \frac{1}{6} (5\mu_{\pi^0} + 3\mu_\eta + 4\mu_{K^0} + 6\mu_{\pi^\pm} + 6\mu_{K^\pm}) \right. \\
&- \frac{8}{F_0^2} \left[2(M_\pi^2 + 2M_K^2)L_4^r + (M_\pi^2 + M_K^2)L_5^r \right] \\
&+ 2e^2 \left[-\frac{1}{8\pi^2} - \frac{1}{16\pi^2} \left(\ln \frac{m_\gamma^2}{M_\pi^2} + \ln \frac{m_\gamma^2}{M_K^2} \right) - 2F_0^2 \tilde{\mu}_\pi - 2F_0^2 \tilde{\mu}_K \right. \\
&- \frac{4}{9}(6K_1^r + 6K_2^r + 5K_5^r + 5K_6^r) \left. \right] - \frac{\epsilon}{\sqrt{3}}(\mu_\eta - \mu_\pi) + \frac{16}{F_0^2} \left(\frac{\epsilon}{\sqrt{3}} \right) (M_K^2 - M_\pi^2)L_5^r \left. \right\} \\
&+ \frac{M_{K^\pm}^2}{6F_0^2} \left\{ -\frac{2}{3}\mu_\eta + \frac{2\epsilon}{\sqrt{3}}(\mu_\eta - \mu_\pi) + \frac{16}{F_0^2} \left(\frac{\epsilon}{\sqrt{3}} \right) (M_K^2 - M_\pi^2)(2L_8^r - L_5^r) \right. \\
&- \frac{8}{F_0^2} \left[(M_\pi^2 + 2M_K^2)(2L_6^r - L_4^r) + M_K^2(2L_8^r - L_5^r) \right] - e^2 \left[\frac{1}{4\pi^2} - 6F_0^2 \tilde{\mu}_K \right. \\
&- \frac{4}{9}(6K_1^r + 6K_2^r + 5K_5^r + 5K_6^r - 6K_7^r - 150K_8^r - 2K_9^r - 20K_{10}^r - 18K_{11}^r) \left. \right] \left. \right\} \\
&+ \frac{M_{\pi^\pm}^2}{6F_0^2} \left\{ -\mu_{\pi^0} + \frac{1}{3}\mu_\eta - \frac{8}{F_0^2} \left[(M_\pi^2 + 2M_K^2)(2L_6^r - L_4^r) + M_\pi^2(2L_8^r - L_5^r) \right] \right. \\
&- e^2 \left[\frac{7}{4\pi^2} - 42F_0^2 \tilde{\mu}_\pi - \frac{4}{9}(6K_1^r + 6K_2^r \right. \\
&+ 54K_3^r - 27K_4^r + 5K_5^r + 5K_6^r - 6K_7^r - 78K_8^r - 8K_9^r - 134K_{10}^r - 126K_{11}^r) \left. \right] \left. \right\} \\
&+ \frac{\Delta_\pi}{6F_0^2} \left\{ \frac{3M_\pi^2}{8\pi^2 F_0^2} + 54\mu_\pi + 28\mu_K + \frac{10}{3}\mu_\eta \right. \\
&+ \frac{16}{F_0^2} \left[-3(M_\pi^2 + 2M_K^2)L_4^r - 3M_K^2 L_5^r + 2(M_\pi^2 + 2M_K^2)L_6^r + (M_\pi^2 + M_K^2)L_8^r \right] \left. \right\} .
\end{aligned} \tag{A.2}$$

As usually, the tadpole integrals read

$$\mu_P = M_P^2 \tilde{\mu}_P = \frac{M_P^2}{32\pi^2 F_0^2} \ln \frac{M_P^2}{\mu^2} ,$$

and the difference between the charged and neutral mesons masses is symbolized by

$$\Delta_P = M_{P^\pm}^2 - M_{P^0}^2 .$$

Note that an infrared divergent piece appears in (A.2). It comes from the charged mesons wave functions renormalization and is regularized by assigning a fictitious mass m_γ to the photon. The counter-terms contribution $\mathcal{M}_{p^4}^{\text{born}}$ issues from the NLO lagrangian of the strong sector [26] and is put in the following form

$$\begin{aligned}
\mathcal{M}_{p^4}^{\text{born}} &= \frac{1}{F_0^4} \sum_{i=1}^8 \mathcal{P}_i L_i^r, \\
\mathcal{P}_1 &= 8(2M_{\pi^\pm}^2 - t)(2M_{K^\pm}^2 - t), \\
\mathcal{P}_2 &= 4 \left[(\Sigma_{\pi^- K^+} - s)^2 + (\Sigma_{\pi^- K^+} - u)^2 \right], \\
\mathcal{P}_3 &= 2(2M_{\pi^\pm}^2 - t)(2M_{K^\pm}^2 - t) + 2(\Sigma_{\pi^- K^+} - s)^2, \\
\mathcal{P}_4 &= -\frac{2}{3} \left[M_\pi^2 + 14M_K^2 - \frac{24\epsilon}{\sqrt{3}}(M_K^2 - M_\pi^2) \right] (2M_{\pi^\pm}^2 - t) - \frac{2}{3}(13M_\pi^2 + 2M_K^2)(2M_{K^\pm}^2 - t) \\
&\quad - \frac{4}{3}(M_\pi^2 + 2M_K^2)(\Sigma_{\pi^- K^+} - s) + \frac{8}{3}(M_\pi^2 + 2M_K^2)(\Sigma_{\pi^- K^+} - u), \\
\mathcal{P}_5 &= -\frac{2}{3}(3M_{\pi^0}^2 + M_{K^\pm}^2 - \Delta_\pi)(2M_{K^\pm}^2 - t) - \frac{2}{3}(M_{\pi^0}^2 + 3M_{K^\pm}^2 - 3\Delta_\pi)(2M_{\pi^\pm}^2 - t) \\
&\quad - \frac{8}{3}(M_{\pi^0}^2 + M_{K^\pm}^2 - \Delta_\pi)(\Sigma_{\pi^- K^+} - s) + \frac{4}{3}(M_{\pi^0}^2 + M_{K^\pm}^2 - \Delta_\pi)(\Sigma_{\pi^- K^+} - u), \\
\mathcal{P}_6 &= \frac{8}{3} \left[2M_K^4 + 15M_\pi^2 M_K^2 + M_\pi^4 - \frac{2\epsilon}{\sqrt{3}}(2M_K^4 + 11M_\pi^2 M_K^2 - 13M_\pi^4) \right], \\
\mathcal{P}_7 &= 0, \\
\mathcal{P}_8 &= \frac{8}{3} \left[M_K^4 + 6M_\pi^2 M_K^2 + M_\pi^4 - \frac{4\epsilon}{\sqrt{3}}(M_K^4 + 2M_\pi^2 M_K^2 - 3M_\pi^4) \right], \tag{A.3}
\end{aligned}$$

where

$$\Sigma_{PQ} = M_P^2 + M_Q^2.$$

Finally, $\mathcal{M}_{e^2 p^2}^{\text{born}}$ represents the counter-terms contribution of $\mathcal{O}(e^2 p^2)$. It springs from the NLO lagrangian in the electromagnetic sector and reads

$$\begin{aligned}
\mathcal{M}_{e^2 p^2}^{\text{born}} &= \frac{2e^2}{27F_0^2} (12K_1^r + 12K_2^r + 54K_3^r + 27K_4^r + 10K_5^r + 10K_6^r)(\Sigma_{\pi K} - u) \\
&\quad - \frac{2e^2}{27F_0^2} (6K_1^r + 6K_2^r + 54K_3^r + 27K_4^r - 4K_5^r + 50K_6^r)(\Sigma_{\pi K} - s) \\
&\quad - \frac{4e^2}{27F_0^2} (3K_1^r + 57K_2^r + 7K_5^r + 34K_6^r)(\Sigma_{\pi K} - t) \\
&\quad + \frac{4e^2}{27F_0^2} \left[3(M_\pi^2 + M_K^2)K_7 + 3(31M_\pi^2 + 43M_K^2)K_8 \right. \\
&\quad \left. + (4M_\pi^2 + M_K^2)K_9 + (94M_\pi^2 + 91M_K^2)K_{10}^r + 90(M_\pi^2 + M_K^2)K_{11}^r \right]. \tag{A.4}
\end{aligned}$$

The tadpole-type part of the amplitude is furnished by diagram (b) in figure 1. Its result is shown by keeping apart individual contributions from each meson loop

$$\mathcal{M}^{\text{tadpole}} = \frac{\mu_{\pi^0}}{36F_0^2} \left[6u - t + 6\Delta_{\pi^- K^+} - 24\Delta_\pi + \frac{2\epsilon}{\sqrt{3}}(3t + 2M_\pi^2 + 4M_K^2) \right]$$

$$\begin{aligned}
& + \frac{\mu_\eta}{36F_0^2} \left[6u - 3t - 6M_{\pi^\pm}^2 + 2M_{K^\pm}^2 - 20\Delta_\pi - \frac{6\epsilon}{\sqrt{3}}(t - 2M_\pi^2 + 4M_K^2) \right] \\
& + \frac{\mu_{\pi^\pm}}{18F_0^2} (12u + 3t - 8M_{\pi^\pm}^2 - 12M_{K^\pm}^2 - 72\Delta_\pi) \\
& + \frac{\mu_{K^0}}{9F_0^2} \left[-2t + 2M_{K^\pm}^2 + M_{\pi^\pm}^2 - 3\Delta_\pi + \frac{4\epsilon}{\sqrt{3}}(M_K^2 - M_\pi^2) \right] \\
& + \frac{\mu_{K^\pm}}{18F_0^2} (12u + 3t - 12M_{\pi^\pm}^2 - 8M_{K^\pm}^2 - 72\Delta_\pi). \tag{A.5}
\end{aligned}$$

Concerning the unitary corrections following from diagram (b) and its two crossed in Fig. 1, they will be separated according to the channel specifying each crossed diagram. Moreover, the contribution of each channel will be divided into parts labelled by the kind of particles propagating inside the loop. For instance, in the s -channel

$$\mathcal{M}^{\text{S-channel}} = \mathcal{M}_{\pi^-K^+}^{\text{s-channel}} + \mathcal{M}_{\pi^0K^0}^{\text{s-channel}} + \mathcal{M}_{\eta K^0}^{\text{s-channel}},$$

where

$$\begin{aligned}
\mathcal{M}_{\pi^-K^+}^{\text{s-channel}} &= \frac{1}{36F_0^4} \left\{ 6F_0^2 \mu_{K^\pm} (s - \Delta_{\pi^-K^+} + 4\Delta_\pi) \right. \\
& + (s + \Delta_{\pi^-K^+} + 6\Delta_\pi)^2 \bar{B}(M_{\pi^\pm}^2, M_{K^\pm}^2; s) \\
& + 2(s - 3\Delta_{\pi^-K^+})(s + \Delta_{\pi^-K^+} + 6\Delta_\pi) \bar{B}_1(M_{\pi^\pm}^2, M_{K^\pm}^2; s) \\
& + (s - 3\Delta_{\pi^-K^+})^2 \bar{B}_{21}(M_{\pi^\pm}^2, M_{K^\pm}^2; s) \\
& \left. + 2s \left[2M_{\pi^\pm}^2 - t + 4(u - t - \Delta_{\pi^-K^+}) \right] \bar{B}_{22}(M_{\pi^\pm}^2, M_{K^\pm}^2; s) \right\}, \\
\mathcal{M}_{\pi^0K^0}^{\text{s-channel}} &= \frac{1}{8F_0^4} \left\{ 2F_0^2 \mu_{K^0} \left(1 + \frac{2\epsilon}{\sqrt{3}} \right) (3s - 3M_{\pi^0}^2 - M_{K^0}^2) \right. \\
& + \left[s - \Sigma_{\pi^0K^0} + \frac{\epsilon}{\sqrt{3}}(s - 9M_\pi^2 + 7M_K^2) \right]^2 \bar{B}(M_{\pi^0}^2, M_{K^0}^2; s) \\
& + 2 \left[s - \Sigma_{\pi^0K^0} + \frac{\epsilon}{\sqrt{3}}(s - 9M_\pi^2 + 7M_K^2) \right] \times \\
& \quad \left[s - \Delta_{\pi^-K^+} + \frac{\epsilon}{\sqrt{3}}(s + 3\Delta_{\pi K}) \right] \bar{B}_1(M_{\pi^0}^2, M_{K^0}^2; s) \\
& + \left[s - \Delta_{\pi^-K^+} + \frac{\epsilon}{\sqrt{3}}(s + 3\Delta_{\pi K}) \right]^2 \bar{B}_{21}(M_{\pi^0}^2, M_{K^0}^2; s) \\
& \left. + 2s \left[2M_{K^\pm}^2 - t + \frac{2\epsilon}{\sqrt{3}}(t - 2u + 2M_\pi^2) \right] \bar{B}_{22}(M_{\pi^0}^2, M_{K^0}^2; s) \right\}, \\
\mathcal{M}_{\eta K^0}^{\text{s-channel}} &= \frac{1}{24F_0^4} \left\{ 2F_0^2 \mu_{K^0} \left(1 - \frac{3\epsilon}{\sqrt{3}} \right) \left[3s - 3M_\eta^2 - M_{K^0}^2 - \frac{3\epsilon}{\sqrt{3}}(3s - M_K^2 - 3M_\eta^2) \right] \right. \\
& + \left[s + 7M_\eta^2 - 9M_{K^0}^2 - \frac{\epsilon}{\sqrt{3}}(3s + 17M_\pi^2 - 23M_K^2) \right]^2 \bar{B}(M_\eta^2, M_{K^0}^2; s) \\
& + 2 \left[s + 3\Delta_{\pi^-K^+} - \frac{3\epsilon}{\sqrt{3}}(s - \Delta_{\pi K}) \right] \times \\
& \quad \left[s + 7M_\eta^2 - 9M_{K^0}^2 - \frac{\epsilon}{\sqrt{3}}(3s + 17M_\pi^2 - 23M_K^2) \right] \bar{B}_1(M_\eta^2, M_{K^0}^2; s) \\
& \left. + \left[s + 3\Delta_{\pi^-K^+} - \frac{3\epsilon}{\sqrt{3}}(s - \Delta_{\pi K}) \right]^2 \bar{B}_{21}(M_\eta^2, M_{K^0}^2; s) \right\}
\end{aligned}$$

$$+ 2s \left[4u - 5t + 4M_{\pi^\pm}^2 - 2M_{K^\pm}^2 - \frac{6\epsilon}{\sqrt{3}}(t - 2u + 2M_\pi^2) \right] \bar{B}_{22}(M_\eta^2, M_{K^0}^2; s) \Big\} . \quad (\text{A.6})$$

The loop functions figuring in (A.6) and in what follows are discussed in Appendix B, the quantity Δ_{PQ} stands for

$$\Delta_{PQ} = M_P^2 - M_Q^2 .$$

Similar notations hold for t - and u -channels

$$\begin{aligned} \mathcal{M}^{t\text{-channel}} &= \mathcal{M}_{\pi^0\pi^0}^{t\text{-channel}} + \mathcal{M}_{\eta\eta}^{t\text{-channel}} + \mathcal{M}_{\pi^0\eta}^{t\text{-channel}} \\ &+ \mathcal{M}_{\pi^+\pi^-}^{t\text{-channel}} + \mathcal{M}_{K^0\bar{K}^0}^{t\text{-channel}} + \mathcal{M}_{K^+K^-}^{t\text{-channel}} , \\ \mathcal{M}^{u\text{-channel}} &= \mathcal{M}_{\pi^-K^+}^{u\text{-channel}} , \end{aligned} \quad (\text{A.7})$$

which individual parts are given by

$$\begin{aligned} \mathcal{M}_{\pi^0\pi^0}^{t\text{-channel}} &= \frac{1}{36F_0^4} \left\{ -2F_0^2\mu_{\pi^0} \left[-5t + 3M_{\pi^0}^2 + \frac{6\epsilon}{\sqrt{3}}(-5t + 3M_\pi^2 + 4M_K^2) \right] \right. \\ &+ \left. \frac{3}{2}(t - M_{\pi^0}^2) \left[3t + \frac{6\epsilon}{\sqrt{3}}(3t - 4M_K^2) \right] \bar{B}(M_{\pi^0}^2, M_{\pi^0}^2; t) \right\} , \\ \mathcal{M}_{\eta\eta}^{t\text{-channel}} &= \frac{M_{\pi^0}^2}{72F_0^4} \left\{ 12F_0^2 \left(1 - \frac{2\epsilon}{\sqrt{3}} \right) \mu_\eta \right. \\ &+ \left. \left[9t - 6M_\eta^2 - 2M_{\pi^0}^2 - \frac{2\epsilon}{\sqrt{3}}(9t + 8M_\pi^2 - 20M_K^2) \right] \bar{B}(M_\eta^2, M_\eta^2; t) \right\} , \\ \mathcal{M}_{\pi^0\eta}^{t\text{-channel}} &= -\frac{1}{12F_0^4} \left(\frac{\epsilon}{\sqrt{3}} \right) \left\{ 2F_0^2\mu_\pi(5t - 6M_\pi^2 - 2M_\eta^2) \right. \\ &+ \left. 2F_0^2\mu_\eta(5t - 4\Sigma_{\pi\eta}) + (3t - 4M_\pi^2)(3t - 3M_\eta^2 - M_\pi^2) \bar{B}(M_\pi^2, M_\eta^2; t) \right\} , \\ \mathcal{M}_{\pi^+\pi^-}^{t\text{-channel}} &= \frac{1}{18F_0^4} \left\{ -\frac{3}{16\pi^2} \left(M_{\pi^\pm}^2 - \frac{t}{6} \right) (s - u) + F_0^2\mu_{\pi^\pm} [5t + 24\Delta_\pi + 3(s - u)] \right. \\ &+ \left. \left[\frac{9}{4}t(t + 8\Delta_\pi) - 3(s - u) \left(M_{\pi^\pm}^2 - \frac{t}{4} \right) \right] \bar{B}(M_{\pi^\pm}^2, M_{\pi^\pm}^2; t) \right\} , \\ \mathcal{M}_{K^0\bar{K}^0}^{t\text{-channel}} &= \frac{1}{36F_0^4} \left\{ F_0^2\mu_{K^0} [5t - 3(s - u)] + \frac{3}{16\pi^2} \left(M_{K^0}^2 - \frac{t}{6} \right) (s - u) \right. \\ &+ \left. \left[\frac{9}{4}t^2 + 3(s - u) \left(M_{K^0}^2 - \frac{t}{4} \right) \right] \bar{B}(M_{K^0}^2, M_{K^0}^2; t) \right\} , \\ \mathcal{M}_{K^+K^-}^{t\text{-channel}} &= \frac{1}{18F_0^4} \left\{ F_0^2\mu_{K^\pm} [5t + 3(s - u) + 24\Delta_\pi] - \frac{3}{16\pi^2} \left(M_{K^\pm}^2 - \frac{t}{6} \right) (s - u) \right. \\ &+ \left. \left[\frac{9}{4}t(t + 8\Delta_\pi) - 3(s - u) \left(M_{K^\pm}^2 - \frac{t}{4} \right) \right] \bar{B}(M_{K^\pm}^2, M_{K^\pm}^2; t) \right\} , \\ \mathcal{M}_{\pi^-K^+}^{u\text{-channel}} &= \frac{1}{9F_0^4} \left\{ -6F_0^2\mu_{K^\pm}(\Sigma_{\pi^-K^+} - u + 2\Delta_\pi) \right. \\ &+ (2M_{\pi^\pm}^2 + M_{K^\pm}^2 - u + 3\Delta_\pi)^2 \bar{B}(M_{\pi^\pm}^2, M_{K^\pm}^2; u) \\ &- 2u(2M_{\pi^\pm}^2 + M_{K^\pm}^2 - u + 3\Delta_\pi) \bar{B}_1(M_{\pi^\pm}^2, M_{K^\pm}^2; u) \\ &+ \left. u^2 \bar{B}_{21}(M_{\pi^\pm}^2, M_{K^\pm}^2; u) + u^2 \bar{B}_{22}(M_{\pi^\pm}^2, M_{K^\pm}^2; u) \right\} . \end{aligned} \quad (\text{A.8})$$

With regard to the one-photon contributions, they will be classified with respect to the topology of the exchanged photon

$$\mathcal{M}^{\text{one-photon}} = \mathcal{M}_{\text{vertex-leg}}^{\text{one-photon}} + \mathcal{M}_{\text{s-channel}}^{\text{one-photon}} + \mathcal{M}_{\text{t-channel}}^{\text{one-photon}} + \mathcal{M}_{\text{u-channel}}^{\text{one-photon}}.$$

We distinguish a tadpole-type contribution schematized by diagram (e) in Fig. 1 and for which we found

$$\mathcal{M}_{\text{vertex-leg}}^{\text{one-photon}} = \frac{2e^2}{3F_0^2} \left[(u + \Delta_{\pi K}) \left(-6F_0^2 \tilde{\mu}_\pi + \frac{1}{4\pi^2} \right) + (u - \Delta_{\pi K}) \left(-6F_0^2 \tilde{\mu}_K + \frac{1}{4\pi^2} \right) \right].$$

We also distinguish a unitary contribution given by diagram (d) in Fig. 1. The expressions relative to the different channels defined by the exchanged photon topology read

$$\begin{aligned} \mathcal{M}_{\text{s-channel}}^{\text{one-photon}} &= \frac{e^2}{3F_0^2} \left\{ \frac{1}{2} F_0^2 \tilde{\mu}_\pi \left[3(t-u) - 12(\Sigma_{\pi K} - u) + s - 2\Delta_{\pi K} \right] \right. \\ &+ \frac{1}{2} F_0^2 \tilde{\mu}_K \left[3(t-u) - 12(\Sigma_{\pi K} - u) + s + 2M_\pi^2 - 6M_K^2 \right] \\ &+ (s - 3M_\pi^2 - M_K^2) \bar{B}(M_\pi^2, M_K^2, s) + (3\Delta_{\pi K} - s) \bar{B}_1(M_\pi^2, M_K^2, s) \\ &+ 2(\Sigma_{\pi K} - s) \left[3(u-t) + 2\Sigma_{\pi K} - s \right] G_{\pi K}^-(s) + 8\Delta_{\pi K} (\Sigma_{\pi K} - s) G_{\pi K}^+(s) \\ &+ \left. 6(\Sigma_{\pi K} - u)(\Sigma_{\pi K} - s) G_{\pi K}(s) + 6(\Sigma_{\pi K} - u) \left(\frac{1}{16\pi^2} \right) \right\}, \\ \mathcal{M}_{\text{t-channel}}^{\text{one-photon}} &= \frac{e^2}{6F_0^2} \left\{ -2F_0^2 \tilde{\mu}_\pi \left[6(\Sigma_{\pi K} - u) - \frac{3}{2}(2M_\pi^2 - t) \right] \right. \\ &- 3(\Sigma_{\pi K} - u) \bar{B}(M_\pi^2, M_\pi^2, t) - \frac{1}{16\pi^2} \left[-9(\Sigma_{\pi K} - u) - \frac{1}{2}(t - 8M_\pi^2) \right] \\ &+ \left. 6(2M_\pi^2 - t)(\Sigma_{\pi K} - u) G_{\pi\pi}(t) - \frac{3}{2}(s-u)(4M_\pi^2 - 3t) G_{\pi\pi}^-(t) \right\} \\ &+ \frac{e^2}{6F_0^2} \left\{ -2F_0^2 \tilde{\mu}_K \left[6(\Sigma_{\pi K} - u) - \frac{3}{2}(2M_K^2 - t) \right] \right. \\ &- 3(\Sigma_{\pi K} - u) \bar{B}(M_K^2, M_K^2, t) - \frac{1}{16\pi^2} \left[-9(\Sigma_{\pi K} - u) - \frac{1}{2}(t - 8M_K^2) \right] \\ &+ \left. 6(2M_K^2 - t)(\Sigma_{\pi K} - u) G_{KK}(t) - \frac{3}{2}(s-u)(4M_K^2 - 3t) G_{KK}^-(t) \right\}, \\ \mathcal{M}_{\text{u-channel}}^{\text{one-photon}} &= -\frac{e^2}{3F_0^2} \left\{ F_0^2 \tilde{\mu}_\pi (5u - 5M_K^2 - 7M_\pi^2) + F_0^2 \tilde{\mu}_K (5u - 5M_\pi^2 - 3M_K^2) \right. \\ &+ 2(M_K^2 - u) \bar{B}(M_\pi^2, M_K^2, u) + 2u \bar{B}_1(M_\pi^2, M_K^2, u) \\ &- 4(\Sigma_{\pi K} - u)(2\Sigma_{\pi K} - u) G_{\pi K}^-(u) - 4\Delta_{\pi K} (\Sigma_{\pi K} - u) G_{\pi K}^+(u) \\ &+ \left. 6(\Sigma_{\pi K} - u)^2 G_{\pi K}(u) + 6(\Sigma_{\pi K} - u) \left(\frac{1}{16\pi^2} \right) \right\}. \end{aligned} \quad (\text{A.9})$$

Finally, the result for diagram (f) in Fig. 1 can be put in the following form

$$\mathcal{M}^{\text{form factor}} = e^2 \left(\frac{u-s}{t} \right) \left[1 + \Gamma_\pi(t) + \Gamma_K(t) \right],$$

where Γ_π and Γ_K represent the electromagnetic vertex functions for the pion and kaon respectively [50]

$$\Gamma_\pi(t) = \frac{t}{F_0^2} \left[2L_9^r - \frac{1}{96\pi^2} \left(\ln \frac{M_\pi^2}{\mu^2} + \frac{1}{2} \ln \frac{M_K^2}{\mu^2} \right) \right]$$

$$\begin{aligned}
& - \frac{2}{3F_0^2} \left[(M_\pi^2 - \frac{t}{4}) \bar{B}(M_\pi^2, M_\pi^2, t) + \frac{1}{16\pi^2} \frac{t}{12} \right] \\
& - \frac{1}{3F_0^2} \left[(M_K^2 - \frac{t}{4}) \bar{B}(M_K^2, M_K^2, t) + \frac{1}{16\pi^2} \frac{t}{12} \right], \\
\Gamma_K(t) & = \frac{t}{F_0^2} \left[2L_9 - \frac{1}{96\pi^2} \left(\ln \frac{M_K^2}{\mu^2} + \frac{1}{2} \ln \frac{M_\pi^2}{\mu^2} \right) \right] \\
& - \frac{1}{3F_0^2} \left[(M_\pi^2 - \frac{t}{4}) \bar{B}(M_\pi^2, M_\pi^2, t) + \frac{1}{16\pi^2} \frac{t}{12} \right] \\
& - \frac{2}{3F_0^2} \left[(M_K^2 - \frac{t}{4}) \bar{B}(M_K^2, M_K^2, t) + \frac{1}{16\pi^2} \frac{t}{12} \right].
\end{aligned} \tag{A.10}$$

B Loop functions

The loop functions we used in our calculations follow the notations of [51] and which analytic expressions were given in [24]. For completeness we recall the expression for the following function

$$\begin{aligned}
\mathcal{B}(x, y) & = -\frac{\sqrt{(x-y)(2x+y)}}{12\pi^2(x+y)} \times \\
& \left\{ \arctan \left[\frac{\sqrt{(x-y)(2x+y)}}{2(x-y)} \right] + \arctan \left[\frac{x+2y}{2\sqrt{(x-y)(2x+y)}} \right] \right\}. \tag{B.1}
\end{aligned}$$

For the threshold expansion of the processes analyzed in this paper, we needed the following expressions for the two-point functions defined in [24]

$$\begin{aligned}
\text{Re } \bar{B}(M_{\pi^\pm}^2, M_{K^\pm}^2, M_\pm^2) & = \frac{1}{16\pi^2} \left(1 \mp \frac{M_{\pi^\pm} M_{K^\pm}}{M_{K^\pm}^2 - M_{\pi^\pm}^2} \ln \frac{M_{\pi^\pm}^2}{M_{K^\pm}^2} \right), \\
\text{Re } \bar{B}(M_{\pi^0}^2, M_{K^0}^2, M_\pm^2) & = \frac{1}{16\pi^2} \left(1 \mp \frac{M_{\pi^\pm} M_{K^\pm}}{M_{K^\pm}^2 - M_{\pi^\pm}^2} \ln \frac{M_{\pi^\pm}^2}{M_{K^\pm}^2} \right) \\
& + \frac{\Delta_\pi}{32\pi^2} \left\{ \frac{2}{M_K^2 - M_\pi^2} \left(2 \mp \frac{M_K}{M_\pi} \right) \right. \\
& + \frac{1}{(M_K^2 - M_\pi^2)^2} [2(2M_K^2 + M_\pi^2) - (M_K \pm M_\pi)^2] \ln \frac{M_\pi^2}{M_K^2} \left. \right\} \\
& - \frac{\Delta_K}{32\pi^2} \left\{ \frac{2}{M_K^2 - M_\pi^2} \left(2 \mp \frac{M_\pi}{M_K} \right) \right. \\
& + \frac{1}{(M_K^2 - M_\pi^2)^2} [2(M_K^2 + 2M_\pi^2) - (M_K \pm M_\pi)^2] \ln \frac{M_\pi^2}{M_K^2} \left. \right\}, \\
\text{Re } \bar{B}(M_\eta^2, M_{K^0}^2, M_\pm^2) & = \frac{1}{16\pi^2} [1 + 16\pi^2 \mathcal{B}(M_{K^\pm}, \pm M_{\pi^\pm})] \\
& + \frac{1}{48\pi^2} \frac{1}{M_{K^\pm}^2 - M_{\pi^\pm}^2} (5M_{K^\pm} \mp 2M_{\pi^\pm})(2M_{K^\pm} \pm M_{\pi^\pm}) \ln \frac{M_\eta^2}{M_{K^\pm}^2} \\
& - \frac{1}{96\pi^2} \frac{\Delta_\pi}{M_K^2 - M_\pi^2} \left[12\pi^2 \left(\frac{M_K \pm 2M_\pi}{2M_K \pm M_\pi} \right) \mathcal{B}(M_K, \pm M_\pi) \right]
\end{aligned}$$

$$\begin{aligned}
& + 2 \left(\frac{M_K \mp M_\pi}{2M_K \mp M_\pi} \right) - \left(\frac{19M_K^2 \mp 2M_K M_\pi + M_\pi^2}{M_K^2 - M_\pi^2} \right) \ln \frac{M_\eta^2}{M_K^2} \Big] \\
& - \frac{1}{96\pi^2} \frac{\Delta_K}{M_K^2 - M_\pi^2} \left[12\pi^2 \left(\frac{8M_K \pm 7M_\pi}{2M_K \pm M_\pi} \right) \mathcal{B}(M_K, \pm M_\pi) \right. \\
& \left. - 2 \left(\frac{16M_K \mp 7M_\pi}{2M_K \mp M_\pi} \right) + \left(\frac{37M_K^2 \mp 2M_K M_\pi - 17M_\pi^2}{M_K^2 - M_\pi^2} \right) \ln \frac{M_\eta^2}{M_K^2} \right],
\end{aligned} \tag{B.2}$$

and evaluated at

$$M_\pm = M_{\pi^\pm} \pm M_{K^\pm}.$$

Finally, we quote the expression of the infrared divergent three-point function with the corresponding cut structure needed for the calculation of diagram (d) in Fig. 1 with the various channels defined in Eq. (A.9)

$$\begin{aligned}
32\pi^2 \lambda_{PQ}^{\frac{1}{2}}(p^2) G_{PQ}(p^2) &= 2 \operatorname{Li}_2 \left[\frac{p^2 + \Delta_{PQ} + \lambda_{PQ}^{\frac{1}{2}}(p^2)}{p^2 + \Delta_{PQ} - \lambda_{PQ}^{\frac{1}{2}}(p^2)} \right] - 2 \operatorname{Li}_2 \left[\frac{p^2 - \Delta_{PQ} - \lambda_{PQ}^{\frac{1}{2}}(p^2)}{p^2 - \Delta_{PQ} + \lambda_{PQ}^{\frac{1}{2}}(p^2)} \right] \\
&- \left\{ \ln \left[\frac{\lambda_{PQ}(p^2)}{p^2 m_\gamma^2} \right] - \frac{1}{2} \ln \left[\frac{[\Delta_{PQ} - \lambda_{PQ}^{\frac{1}{2}}(p^2)]^2 - p^4}{[\Delta_{PQ} + \lambda_{PQ}^{\frac{1}{2}}(p^2)]^2 - p^4} \right] - i\pi \Theta(p^2) \right\} \times \\
&\left\{ \ln \left[\frac{[p^2 - \lambda_{PQ}^{\frac{1}{2}}(p^2)]^2 - \Delta_{PQ}^2}{[p^2 + \lambda_{PQ}^{\frac{1}{2}}(p^2)]^2 - \Delta_{PQ}^2} \right] + 2i\pi \Theta [p^2 - (M_P + M_Q)^2] \right\}.
\end{aligned} \tag{B.3}$$

In this expression, Θ stands for the Heaviside function, λ_{PQ} the Lehmann function

$$\lambda_{PQ}(p^2) \equiv [p^2 - (M_P + M_Q)^2] [p^2 - (M_P - M_Q)^2],$$

and the dilogarithm function is defined as

$$\operatorname{Li}_2(z) \equiv - \int_0^z dt \frac{\ln(1-t)}{t}.$$

Notice that in the equal mass limit ($M_P = M_Q$), the function (B.3) reduces to the one given in [20].

References

- [1] B. Adeva *et al.*, CERN-SPSLC-95-1.
- [2] D. Sigg, A. Badertscher, P. F. Goudsmit, H. J. Leisi and G. C. Oades, Nucl. Phys. A **609** (1996) 310;
H. J. Leisi, PiN Newslett. **15** (1999) 258;
H. C. Schroder *et al.*, Phys. Lett. B **469** (1999) 25;
D. Gotta, PiN Newslett. **15** (1999) 276.

- [3] W. H. Breunlich *et al.* [DEAR Collaboration], PiN Newslett. **15** (1999) 266;
M. Augsburger *et al.*, Nucl. Phys. A **663** (2000) 561.
- [4] M. Iwasaki *et al.*, Phys. Rev. Lett. **78** (1997) 3067;
M. Iwasaki *et al.*, Nucl. Phys. A **639** (1998) 501.
- [5] B. Adeva *et al.*, CERN-SPSC-2000-032.
- [6] S. Deser, M. L. Goldberger, K. Baumann and W. Thirring, Phys. Rev. **96** (1954) 774.
- [7] S. M. Bilenkii, V. H. Nguyen, L. L. Nemenov and F. G. Tkebuchava, Yad. Fiz. **10** (1969) 812.
- [8] H. Leutwyler, Annals Phys. **235** (1994) 165.
- [9] G. Ecker, Prog. Part. Nucl. Phys. **35** (1995) 1.
- [10] A. Pich, “Effective field theory”, in *Les Houches Summer School in Theoretical Physics, Session 68: Probing the Standard Model of Particle Interactions*, R. Gupta, A. Morel, E. de Rafael and F. David Eds., Elsevier, Amsterdam (1999); hep-ph/9806303.
- [11] G. Colangelo, J. Gasser and H. Leutwyler, Phys. Lett. B **488** (2000) 261.
- [12] U. Moor, G. Rasche and W. S. Woolcock, Nucl. Phys. A **587** (1995) 747.
- [13] A. Gashi, G. Rasche, G. C. Oades and W. S. Woolcock, Nucl. Phys. A **628** (1998) 101.
- [14] H. Jallouli and H. Sazdjian, Phys. Rev. D **58** (1998) 014011 [Erratum-ibid. D **58** (1998) 099901];
H. Sazdjian, Phys. Lett. B **490** (2000) 203.
- [15] V. E. Lyubovitskij and A. Rusetsky, Phys. Lett. B **389** (1996) 181;
V. E. Lyubovitskij, E. Z. Lipartia and A. G. Rusetsky, Pisma Zh. Eksp. Teor. Fiz. **66** (1997) 747 [JETP Lett. **66** (1997) 783];
M. A. Ivanov, V. E. Lyubovitskij, E. Z. Lipartia and A. G. Rusetsky, Phys. Rev. D **58** (1998) 094024.
- [16] X. Kong and F. Ravndal, Phys. Rev. D **59** (1999) 014031;
X. w. Kong and F. Ravndal, Phys. Rev. D **61** (2000) 077506;
B. R. Holstein, Phys. Rev. D **60** (1999) 114030;
D. Eiras and J. Soto, Nucl. Phys. Proc. Suppl. **86** (2000) 267 [PiN Newslett. **15** (2000) 181];
D. Eiras and J. Soto, Phys. Rev. D **61** (2000) 114027.
- [17] J. Gasser, V. E. Lyubovitskij, A. Rusetsky and A. Gall, Phys. Rev. D **64** (2001) 016008.
- [18] J. Gasser, V. E. Lyubovitskij and A. Rusetsky, Phys. Lett. B **471** (1999) 244.
- [19] A. Gall, J. Gasser, V. E. Lyubovitskij and A. Rusetsky, Phys. Lett. B **462** (1999) 335.
- [20] M. Knecht and R. Urech, Nucl. Phys. B **519** (1998) 329.
- [21] L. L. Nemenov and V. D. Ovsyannikov, Phys. Lett. B **514** (2001) 247.

- [22] G. V. Efimov, M. A. Ivanov and V. E. Lyubovitskij, Sov. J. Nucl. Phys. **44** (1986) 296 [Yad. Fiz. **44** (1986) 460].
- [23] M. Knecht and A. Nehme, in preparation.
- [24] A. Nehme and P. Talavera, hep-ph/0107299.
- [25] B. Kubis and U. G. Meissner, hep-ph/0107199.
- [26] J. Gasser and H. Leutwyler, Nucl. Phys. B **250** (1985) 465.
- [27] R. Urech, Nucl. Phys. B **433** (1995) 234.
- [28] H. Neufeld and H. Rupertsberger, Z. Phys. C **68** (1995) 91;
H. Neufeld and H. Rupertsberger, Z. Phys. C **71** (1996) 131.
- [29] A. Denner, Fortsch. Phys. **41** (1993) 307.
- [30] S. Weinberg, Phys. Rev. Lett. **17** (1966) 616.
- [31] J. A. Cronin, Phys. Rev. **161** (1967) 1483;
R. W. Griffith, Phys. Rev. **176** (1968) 1705.
- [32] M. Knecht, H. Sazdjian, J. Stern and N. H. Fuchs, Phys. Lett. B **313** (1993) 229.
- [33] A. Roessl, Nucl. Phys. B **555** (1999) 507.
- [34] V. Bernard, N. Kaiser and U. G. Meissner, Phys. Rev. D **43** (1991) 2757;
V. Bernard, N. Kaiser and U. G. Meissner, Nucl. Phys. B **357** (1991) 129.
- [35] M. Gell-Mann, Phys. Rev. **125** (1962) 1067;
S. Okubo, Prog. Theor. Phys. **27** (1962) 949.
- [36] B. R. Holstein, Phys. Lett. B **244** (1990) 83.
- [37] H. Leutwyler and M. Roos, Z. Phys. C **25** (1984) 91.
- [38] N. H. Fuchs, M. Knecht and J. Stern, Phys. Rev. D **62** (2000) 033003.
- [39] G. Amoros, J. Bijnens and P. Talavera, Nucl. Phys. B **602** (2001) 87.
- [40] G. 't Hooft, Nucl. Phys. B **72** (1974) 461;
E. Witten, Nucl. Phys. B **160** (1979) 57.
- [41] L. Rosselet *et al.*, Phys. Rev. D **15** (1977) 574.
- [42] P. Truol, hep-ex/0012012.
- [43] L. L. Nemenov, Sov. J. Nucl. Phys. **41** (1985) 629 [Yad. Fiz. **41** (1985) 980].
- [44] G. V. Efimov, M. A. Ivanov and V. E. Lyubovitskij, JETP Lett. **45** (1987) 672 [Pisma Zh. Eksp. Teor. Fiz. **45** (1987) 526].
- [45] A. A. Belkov, V. N. Pervushin and F. G. Tkebuchava, Yad. Fiz. **44** (1986) 466 [Sov. J. Nucl. Phys. **44** (1986) 300].

- [46] R. F. Dashen, Phys. Rev. **183** (1969) 1245.
- [47] J. Bijnens and J. Prades, Nucl. Phys. B **490** (1997) 239.
- [48] J. Bijnens, Phys. Lett. B **306** (1993) 343.
- [49] R. Baur and R. Urech, Nucl. Phys. B **499** (1997) 319.
- [50] J. Gasser and H. Leutwyler, Nucl. Phys. B **250** (1985) 517.
- [51] G. Passarino and M. J. Veltman, Nucl. Phys. B **160** (1979) 151.